

CODEN STJSAO
ZX470/1381ISSN 0562-1887
UDK 532.629.122.5*629.123.4(043.3)629.5:621.43(075.8)

Performance Simulation of Marine Slow-Speed Diesel Propulsion Engine With Turbocharger Under Aggravated Conditions

Vladimir MEDICA¹⁾, Nikola RAČIĆ²⁾ and
Gojmir RADICA³⁾

- 1) Tehnički fakultet Sveučilišta u Rijeci,
(Faculty of Engineering University of Rijeka),
Vukovarska 58, HR - 51000 Rijeka
Republic of Croatia
- 2) Pomorski fakultet Sveučilišta u Splitu,
(Faculty of Maritime Studies University of
Split),
Zrinsko-Frankopanska 38, HR - 21000 Split
Republic of Croatia
- 3) Contek d.o.o.,
Don Frane Bulića 171,
HR - 21210 Solin,
Republic of Croatia

nikola.racic@pfst.hr

Keywords

*Diesel engine
Ship's propulsion
Simulation
Turbocharging*

Ključne riječi

*Dizelski motor
Prednabijanje
Propulzija broda
Simulacija*

Received (primljeno): 2008-10-15

Accepted (prihvaćeno): 2009-04-23

Original scientific paper

The paper elaborates a mathematical model forming the basis for a computer-simulated model for a diesel propulsion engine. The model is applied in the analysis of steady and transient operating conditions of a turbocharged slow-speed diesel propulsion engine and a fixed blade propeller. Special attention has been paid to examining the stability and availability under aggravated operating conditions such as difficulties in scavenging and turbocharging system. The analysis of the results has established ultimate limits of affecting features and has defined safe operating conditions, in particular those of the turbocharging system. The analyses and the model can be used in finding better design characteristics and in expert operating systems which can analyse different conditions of the system beforehand and offer optimum operating conditions in order to prevent unwanted occurrences.

Simulacija rada broskog sporohodnog dizelskog propulzijskog motora s turbopuhalom u otežanim uvjetima

Izvorno znanstveni članak

Unutar rada prikazan je matematički model na osnovi kojeg je izrađen računalno-simulacijski model broskog propulzijskog dizelskog motora. Model je primijenjen za analizu stacionarnih i dinamičkih uvjeta rada, sporohodnog propulzijskog dizelskog motora s prednabijanjem i broskog vijčanog propulzora s nepomičnim krilima. Posebno je ispitana stabilnost i raspoloživost u otežanim uvjetima rada, kao što su poteškoće u radu sustava ispiranja i prednabijanja cilindara. Analizom rezultata utvrđene su krajnje granice utjecajnih značajki, određena su sigurna pogonska stanja, a posebno sustava turbopuhala. Analize i model mogu poslužiti za pronalaženje poboljšanja konstrukcijskih značajki, i za ekspertne sustave upravljanja, koji mogu unaprijed analizirati različita stanja sustava i ponuditi optimalne uvjete rada kako bi se preduhitriili neželjeni kvarovi.

1. Introduction

Turbocharged slow-speed two-stroke diesel engines are the most common marine propulsion engines today. Such engines drive the ship's propeller directly and in this way create the most efficient propulsion systems. In addition to high performance and reliability, their features include a planned maintenance system carried out exclusively by the crew. The development of these engines aims to increase their specific output, increase their mean effective pressure and the turbocharging

pressure. This has been paralleled by increasingly strict environment preservation standards, so that particular attention has been paid to the processes occurring in the engine cylinders. The turbocharger should ensure enough amount of air, even at transient regimes of operation and particular problems are aggravated conditions, which are well described by Heim [1]. Transient phenomena, caused by significant load changes that can take place under aggravated sailing conditions, result in incomplete combustion and/or exposure of engine parts to overheat. Soot can be expected as well. Besides its adverse impact

Symbols/Oznake

| | | | |
|---------------|--|-----------------------------|--|
| A | - area, m ² - površina | t | - time, s - vrijeme |
| α | - heat transfer coefficient, J/(m ² ·s·K) - koeficijent prijelaza topline | T | - temperature, K - temperatura |
| A_{TD} | - flow area of the turbocharger turbine diffuser, m ² - protočna površina difuzora turbopuhala | T_I | - integration constant - konstanta integracije |
| A_{TL} | - flow area of the turbocharger turbine blade, m ² - protočna površina na lopaticama turbine turbopuhala | T_D | - derivation constant - konstanta derivacije |
| $A_{T, geom}$ | - geometrical flow area of the turbine, m ² - geometrijska protočna površina turbine | u | - specific internal energy, J/kg - specifična unutarnja energija |
| A, B, C | - coefficient - koeficijent | V | - volume, m ³ - obujam |
| c_m | - mean piston speed, m/s - srednja stapna brzina | W | - work, J - rad |
| c_p | - specific heat at $p=const.$, J/(kg·K) - specifični toplinski kapacitet pri $p=const.$ | x | - relative part of the heat released during fuel combustion - relativni dio topline oslobođen za vrijeme izgaranja goriva |
| h | - specific enthalpy, J/kg - specifična entalpija | $y_{(s)}$ | - measured value - mjerena veličina |
| H_d | - fuel lower heat value, J/kg - donja ogrijevna moć goriva | z | - number of cylinders - broj cilindara |
| J | - moment of inertia, kg·m ² - moment inercije | η | - efficiency - efikasnost |
| k | - concentration of the combusted fuel - koncentracija izgoranog goriva | k | - adiabatic exponent - eksponent adijabate |
| K_r | - gain constant - konstanta pojačanja | λ | - air excess ratio - pretičak zraka |
| L_{st} | - stoichiometric air mass, kg/kg - proračunata masa zraka | λ_m | - ratio r/l of the cranking linkage - omjer r/l poluzja |
| m | - mass, kg - masa | π | - pressure ratio, Ludolf number - omjer tlakova, Ludolfov broj |
| m | - Vibe's exponent - Vibe-ov eksponent | τ | - engine stroke number - taktnost motora |
| \dot{m} | - mass flow, kg/s - maseni protok | φ | - crank angle, ° - kut koljena |
| M | - torque, N·m - moment | ψ | - flow function - funkcija protjecanja |
| n | - revolution speed, min ⁻¹ - brzina vrtnje | X_R | - set point - postavljena vrijednost |
| p | - pressure, Pa (bar) - tlak | Subscripts / Indeksi | |
| Q | - heat, J - toplina | a | - ambient state - stanje okoline |
| R | - gas constant, J/(kg·K) - plinska konstanta | c | - cylinder - cilindar |
| s | - Laplace operator - Laplace-ov operator | e | - effective - efektivno |

| | | | |
|----------|--|-----|---|
| g | - fuel - gorivo | pP | - before the compressor - prije puhala |
| geom | - geometrical - geometrijski | pr | - process - proces |
| RZ | - air cooler - rashladnik zraka | pT | - before the turbine - prije turbine |
| <i>i</i> | - exhaust, index - ispušni, indeks | s | - stroke - stapaj |
| IK | - exhaust receiver - ispušni kolektor | st | - wall - stijenka |
| Ind | - indicated - indicirani | T | - turbine - turbina |
| Izg | - combustion - izgaranje | TI | - combustion period - trajanje izgaranja |
| <i>j</i> | - index - indeks | TP | - turbocharger - turbopuhalo |
| K | - receiver - kolektor | tr | - friction - trenje |
| kan | - channel - kanal | u | - suction - usis |
| M | - engine - motor | v | - valve, channel - ventil, kanal |
| o | - nominal operating point - nominalna radna točka | VIT | - variable injection time - promjenjivo vrijeme ubrizgavanja |
| od | - released - odvedena | z | - air - zrak |
| P | - compressor - puhalo | ZP | - ignition delay - kašnjenje paljenja |
| PI | - start of combustion - početak izgaranja | ZU | - injection delay - kašnjenje ubrizgavanja |

on the environment, soot can settle in the exhaust gas passages and lead to fire. The availability of the system, with regard to the output or any other feature, is defined by calculations and confirmed by empirical-experimental methods. In such analyses, computer-aided simulation models are of particular importance.

This paper presents an open non-stationary thermodynamic model for a slow-speed diesel engine, with non-stationary gas dynamic effects being ignored and with an assumed balance of the condition changes in control volumes. The computer-aided simulation model has been designed using the computer application MATLAB 7.0.4. – SIMULINK. The mathematical model is zero-dimensional, and the mathematical descriptions of the individual components stem from the basic laws of mechanics, thermodynamics, heat transfer and fluid dynamics, mutually correlated by conservation laws for mass and energy. The crank angle change and real time have been defined with the help of the simulation time, so that all calculated condition values can be

observed through the crank angle and time respectively. The complete model has been tested by comparison of experimental data for a propulsion system with the slow-speed diesel engine manufactured by MAN B&W, type code 6S50MC, in the doctoral thesis by Račić [2]. The simulation model is based on the models which have been developed and described by Medica [3] and Radica [4].

This paper analyses the engine's performance when the external load is changed due to sailing in heavy seas, and in aggravated conditions of the turbocharging system operation. The impacts of various air temperatures at the suction portion of the compressor as well as the impact of the turbine's contamination have been examined in detail. The combinations of aggravated working conditions have been determined in which the utmost surge limits of the compressor's performance have been reached, thus making a significant contribution which can serve as the basis for upgrading the regulation and safety system of a propulsion engine with regard to the accentuated problems in the turbocharging system.

2. Mathematical model

The model described in this paper is an open non-stationary thermodynamic system in which gas dynamic effects have been neglected and the balance of the condition change in control volumes has been assumed. It is a so-called quasi-steady model. The engine is an open system featuring inlet flows of air, fuel, coolant and loads, as well as outlet flows of exhaust gases, coolant and mechanical energy. The elements of the marine propulsion system with the slow-speed two-stroke diesel engine are: cylinders, exhaust and scavenge air receivers, air cooler, turbine, compressor, engine mechanism, governor, and ship's propeller as the consumer.

The mathematical model is derived from physical laws applied to the processes occurring within the elements of the system.

2.1. Model for the diesel engine cylinder

The variation in thermal energy exchanged between the working fluid and the system boundaries has been defined with the fuel combustion heat and the heat that is transferred to the walls and environment:

$$\frac{dQ}{d\varphi} = \frac{dQ_g}{d\varphi} + \frac{dQ_{od}}{d\varphi} + h_u \frac{dm_u}{d\varphi} + h_i \frac{dm_i}{d\varphi} + h_p \frac{dm_p}{d\varphi}. \quad (1)$$

The equation referring to the temperature change related to crank angle is:

$$\frac{dT_c}{d\varphi} = \frac{\frac{1}{m} \left[-\frac{p \cdot dV}{d\varphi} + \sum_i \frac{dQ_i}{d\varphi} + \sum_j \left(h \frac{dm}{d\varphi} \right)_j \right] - \left[-u \frac{dm}{d\varphi} - m \left(\frac{\partial u}{\partial \lambda} \right) \frac{d\lambda}{d\varphi} - C \right]}{\frac{\partial u}{\partial T} + \frac{A}{B} \frac{p}{T} \frac{\partial u}{\partial p}}, \quad (2)$$

where:

$$A = 1 + \frac{T}{R} \frac{\partial R}{\partial T}, \quad B = 1 - \frac{p}{R} \frac{\partial R}{\partial p},$$

$$C = \frac{p}{B} \frac{\partial u}{\partial p} \left[\frac{1}{m} \frac{dm}{d\varphi} - \frac{1}{V} \frac{dV}{d\varphi} + \frac{1}{R} \left(\frac{\partial R}{\partial \lambda} \right) \frac{d\lambda}{d\varphi} \right].$$

The work carried out in the cylinder is:

$$\frac{dW_c}{d\varphi} = P_c \frac{dV_c}{d\varphi}. \quad (3)$$

The pressure in the cylinder derives from the gas state equation:

$$P_c = \frac{m_c \cdot T_c \cdot R_c}{V_c}, \quad R_c = f(p_c, T_c, \lambda_c). \quad (4)$$

The change of the cylinder volume is determined from the crank mechanism kinematics.

$$\frac{dV_c}{d\varphi} = \frac{V_s}{2} \left[\sin \varphi + \lambda_m \frac{\sin \varphi \cdot \cos \varphi}{\sqrt{1 - \lambda_m^2 \cdot \sin^2 \varphi}} \right]. \quad (5)$$

2.2. Heat transfer from the cylinder walls

According to Hohenberg [5], the coefficient of the heat transfer in the engine cylinder is determined using the equations:

$$\frac{dQ_{st}}{d\varphi} = \sum_{i=1}^n \alpha_c \cdot A_{st,i} (T_{st,i} - T_c) \frac{dt}{d\varphi}, \quad (6)$$

$$\alpha_c = C_1 V_c^{-0.06} p_c^{0.8} T_c^{-0.4} (c_m + C_2)^{0.8}. \quad (7)$$

2.3. Model for the calculation of the combustion

The heat release rate during fuel combustion is:

$$Q_g = f(\varphi) = x_g \cdot m_g \cdot H_d \cdot \eta_{izg}. \quad (8)$$

This paper uses the analytic form of the combustion function according to Vibe, where the process of the combustion is divided into two parts:

$$x_g = x_{g1}(\varphi) + x_{g2}(\varphi), \quad (9)$$

$$x_{g1}(\varphi) = 1 - \exp \left(-C \left(\frac{\varphi - \varphi_{PI}}{\varphi_{TI}} \right)^{m_1+1} \right), \quad (10)$$

$$x_{g2}(\varphi) = 1 - \exp \left(-C \left(\frac{\varphi - \varphi_{PI}}{\varphi_{TI}} \right)^{m_2+1} \right). \quad (11)$$

Where: $C = 6,901$ (for 99,9 % of fuel combustion efficiency).

According to Woschni and Anisits [6], Vibe's exponent depends on the ignition delay, mass of the working fluid, and the engine speed, as defined by equation (12), whereas the variation in combustion period is set by the equation (13).

$$m = m_0 \left(\frac{\Delta\varphi_{ZP,0}}{\Delta\varphi_{ZP}} \right)^{0.5} \left(\frac{P_c \cdot T_{c,0}}{P_{c,0} \cdot T_c} \right) \left(\frac{n_{M,0}}{n_M} \right)^{0.3}, \quad (12)$$

$$\Delta\varphi_{TI} = \Delta\varphi_{TI,0} \left(\frac{\lambda_0}{\lambda} \right)^{0.6} \left(\frac{n_M}{n_{M,0}} \right)^{0.5}. \quad (13)$$

The equation according to Sitkei is used for calculation of the ignition delay [7]:

$$\Delta\varphi_{ZP} = 0,5 + \exp\left(\frac{3,92782}{T_{c,ZP}}\right) \cdot (0,1332 \cdot p_{c,ZP}^{-0,7} + 4,637 \cdot p_{c,ZP}^{-1,8}) \quad (14)$$

During combustion there is no mass exchange between the cylinder and the environment, therefore:

$$\frac{dm_c}{d\varphi} = \frac{dm_{g,c}}{d\varphi} = \frac{dx_g}{d\varphi} m_{g,pr} \quad (15)$$

$$\frac{d\lambda_c}{d\varphi} = -\frac{\lambda_c \cdot dm_{g,c}}{m_{g,c} \cdot d\varphi} \quad (16)$$

2.4. Model for the working fluid exchange process

When modelling the thermodynamic process at the gas exchange period within the engine, the gas flow through the scavenge ports and the exhaust valve should be determined. The quasi-stationary flow is assumed. There is no combustion during the working fluid exchange. The gas flow can be calculated with the aid of a continuity equation for the stationary flow:

$$\frac{dm}{d\varphi} = \alpha_v \cdot A_{v,geom} \cdot \psi \cdot p_1 \sqrt{\frac{2}{R_1 T_1} \frac{dt}{d\varphi}} \quad (17)$$

where:

$$\psi = \sqrt{\frac{\kappa}{\kappa-1} \left[\left(\frac{p_2}{p_1}\right)^{\frac{2}{\kappa}} - \left(\frac{p_2}{p_1}\right)^{\frac{\kappa+1}{\kappa}} \right]} \quad \text{for} \quad (18)$$

$$1 \geq \frac{p_2}{p_1} \geq \left(\frac{2}{\kappa+1}\right)^{\frac{\kappa}{\kappa-1}},$$

$$\psi = \left(\frac{2}{\kappa+1}\right)^{\frac{1}{\kappa-1}} \sqrt{\frac{\kappa}{\kappa+1}} \quad \text{for} \quad \frac{p_1}{p_2} \geq \left(\frac{\kappa+1}{2}\right)^{\frac{\kappa}{\kappa-1}} \quad (19)$$

The variation in air excess ratio due to gases entering from a receiver marked with index *i* occurs only during gas inlet and it is:

$$\frac{d\lambda_c}{d\varphi} = \frac{\frac{dm_{c,i}}{d\varphi} \left(1 - \frac{m_c \cdot m_{g,c,i}}{m_{g,c} \cdot m_{c,i}}\right)}{L_{st} \cdot m_{g,c}} = \frac{\frac{dm_{c,i}}{d\varphi} \left(1 - \frac{\lambda_c \cdot L_{st} + 1}{\lambda_i \cdot L_{st} + 1}\right)}{L_{st} \cdot m_{g,c}} \quad (20)$$

The variation of combusted fuel mass in the cylinder during the scavenging process is:

$$\frac{dm_{g,c}}{d\varphi} = \frac{dm_{c,i}}{d\varphi} \frac{1}{\lambda_i \cdot L_{st} + 1} \quad (21)$$

The working fluid exhaust from the two-stroke engine cylinder with uniflow scavenging starts with the opening of the exhaust valve. The scavenging process starts when the scavenge ports open. The variation in fuel mass during the scavenging process is defined according to equation (22), by the difference of the exhaust gases leaving through the exhaust valve and the air entering through the scavenge ports.

$$\left(\frac{dm_g}{d\varphi}\right)_{IRM} = k_u \frac{dm_u}{d\varphi} - k_i \frac{dm_i}{d\varphi} \quad (22)$$

The concentration of the combusted fuel in inlet and exhaust gases depends on the type of scavenging. In this paper, the scavenging model has been designed in compliance with the Benson-Brandham model [8], which describes scavenging as a combination of displacement and mixing, with the possibility of short circuiting of the fresh charge directly through the exhaust valve.

2.5. Model for the scavenge air receiver and exhaust gas receiver

Quasi-stationary calculation has been applied, i.e. only the pressure variation through time is taken into consideration, excluding the variation through space of the receiver. Heat transfer between gases and the receiver's walls has been taken into consideration when designing the receiver.

In accordance with the calculation of the cylinder space, the following equations can be applied for the receivers:

$$\frac{dQ_{g,K}}{d\varphi} = \frac{dV_K}{d\varphi} = 0, \quad (23)$$

$$\frac{dT_K}{d\varphi} = \frac{1}{m_K \left(\frac{\partial u}{\partial T}\right)_K} \left[\frac{dQ_{st,K}}{d\varphi} - u_K \frac{dm_K}{d\varphi} + \sum_i h_i \frac{dm_{K,i}}{d\varphi} - m_K \left(\frac{\partial u}{\partial \lambda}\right)_{UK} \frac{d\lambda_K}{d\varphi} \right] \quad (24)$$

$$\frac{d\lambda_{IK}}{d\varphi} = \frac{\sum_i \frac{dm_{IK,i}}{d\varphi} \left(1 - \frac{\lambda_{IK} \cdot L_{st} + 1}{\lambda_i \cdot L_{st} + 1}\right)}{L_{st} \cdot m_{g,IK}} \quad (25)$$

Convective heat transfer from the gases to the walls takes place in the receiver.

$$\begin{aligned} \frac{dQ_K}{d\varphi} &= \alpha_K \cdot A_K \cdot (T_{st,K} - T_K) \frac{dt}{d\varphi} + \\ &+ \alpha_{kan} \cdot A_{kan} \cdot (T_{st,kan} - T_K) \frac{dt}{d\varphi}. \end{aligned} \quad (26)$$

In a tubular receiver as well as in laminar and turbulent flows, the heat transfer coefficient is calculated according to Boy [9]. Heat conductivity and dynamic viscosity of the exhaust gases are calculated according to Pflaum [10].

2.6. Air cooler

The cooler is observed as a damping component featuring an intense withdrawal of heat.

Air temperatures at the cooler's inlet and outlet are:

$$\begin{aligned} T_1 &= T_o + \frac{T_o}{\eta_p} \left(\pi_p^{\frac{\kappa-1}{\kappa}} - 1 \right), \\ T_2 &= T_1 - (T_1 - T_{v2}) \frac{1 - \exp \left[\left(\frac{C_z}{C_v} - 1 \right) \frac{(A_{RZ} \cdot k_{RZ})}{C_z} \right]}{1 - \frac{C_z}{C_v} \exp \left[\left(\frac{C_z}{C_v} - 1 \right) \frac{(A_{RZ} \cdot k_{RZ})}{C_z} \right]}. \end{aligned} \quad (27)$$

where:

$$C_z = c_{p,z} \frac{dm_z}{dt}, \quad C_v = c_{p,v} \frac{dm_v}{dt}.$$

Air pressure after the cooler is:

$$p_2 = p_1 - \Delta p_o \left(\frac{dm_p}{dt} \frac{dt}{dm_{p,o}} \right)^2. \quad (28)$$

2.7. Model for the exhaust gas turbine

Mass flow of the turbine can be established by the equation (29):

$$\frac{dm_T}{d\varphi} = \alpha_T \cdot A_{T,geom} \cdot \psi \cdot p_{IK} \sqrt{\frac{2}{R_{IK} \cdot T_{IK}}} \frac{dt}{d\varphi}. \quad (29)$$

where: $A_{T,geom} = \frac{A_{TD} \cdot A_{TL}}{\sqrt{A_{TD}^2 + A_{TL}^2}}$ is the geometric section of

the turbine, α_T the flow coefficient, ψ flow function which is calculated following the equations (18 and 19).

Isentropic turbine power in the stationary regime is:

$$P_{IS,T} = \dot{m}_T \cdot \Delta h_{s,T}. \quad (30)$$

For ideal gas having constant specific heat during expansion in the turbine, the specific isentropic enthalpy drop is:

$$\Delta h_{s,T} = R_{IK} \frac{\kappa_{IK}}{\kappa_{IK} - 1} \left[1 - \left(\frac{1}{\pi_T} \right)^{\frac{\kappa_{IK} - 1}{\kappa_{IK}}} \right]. \quad (31)$$

where: $\pi = \frac{p_{T,pT}}{p_{T,nT}}$ is the expansion ratio in the turbine.

Internal isentropic efficiency is defined by the ratio between the internal and isentropic work:

$$\eta_T = \frac{\Delta h_T}{\Delta h_{s,T}}. \quad (32)$$

The flow coefficient α_T and the isentropic efficiency η_T are functions of the pressure ratio π_T and speed ratio u/c_o . They depend on the geometric features of the turbine. For the purposes of this paper, the features have been acquired through the digitisation of diagrams provided by the manufacturer.

2.8. Model for the compressor

Mass flow of the turbine can be determined following the equation:

$$\frac{dm_p}{d\varphi} = \frac{dV_{1,288}}{dt} \sqrt{\frac{T_o}{T_a}} \frac{P_a}{R_a T_a} \frac{dt}{d\varphi}. \quad (33)$$

The specific isentropic enthalpy drop is:

$$\Delta h_{s,P} = \frac{\kappa_{zp,P}}{\kappa_{zp,P} - 1} R_{zp,P} \cdot T_{zp,P} \left[\pi_P^{\frac{\kappa_{zp,P}}{\kappa_{zp,P} - 1}} - 1 \right]. \quad (34)$$

As it is hard to get the features in an analytic form from the turbocharger manufacturer, it is necessary to carry out an approximate valuation of the characteristic of the air flow through the compressor and the efficiency in the function of the pressure ratio and revolution speed. For the purposes of this paper the above mentioned features have been acquired through the digitisation of diagrams provided by the manufacturer.

2.9. Dynamics of the turbocharger rotor

During the non-stationary regime of engine operation there is a difference in torque between the turbine and compressor, so that the rotor will speed up or slow down. The change of revolution speed is defined by the difference between torque and moment of inertia:

$$\frac{dm_{TP}}{dt} \frac{dt}{d\varphi} = \frac{M_T - M_P}{J_{TP}} \frac{60}{2 \cdot \pi} \frac{dt}{d\varphi} = \frac{M_T - M_P}{6 \cdot n_M \cdot J_{TP}} \frac{30}{\pi}. \quad (35)$$

The torque of the turbine and compressor can be determined from the turbine and compressor's operation:

$$M_T = \frac{dW_T}{dt} \frac{60}{2 \cdot \pi \cdot n_{TP}} = \frac{dm_T}{d\varphi} \Delta h_{s,T} \cdot \eta_T \frac{60}{2 \cdot \pi \cdot n_{TP}} \frac{d\varphi}{dt}, \quad (36)$$

$$M_P = \frac{dW_P}{dt} \frac{60}{2 \cdot \pi \cdot n_{TP}} = \frac{dm_P}{d\varphi} \frac{\Delta h_{s,P}}{\eta_P \cdot \eta_{meh} \cdot \eta_{vol}} \frac{60}{2 \cdot \pi \cdot n_{TP}} \frac{d\varphi}{dt}. \quad (37)$$

2.10. Dynamics of engine mechanism

The change of revolution speed is:

$$\frac{dn_M}{d\varphi} = \frac{M_M + M_V}{J_M + J_V} \frac{30}{\pi} \frac{dt}{d\varphi} = \frac{P_M + P_V}{6 \cdot n_M^2 (J_M + J_V)} \left(\frac{30}{\pi} \right)^2. \quad (38)$$

Indicated engine power can be calculated on the basis of developed work in the engine cylinder:

$$P_{Ind} = \frac{n_M \cdot z}{30 \cdot \tau} \int \frac{dW_c}{d\varphi} d\varphi. \quad (39)$$

The effective engine power P_{M^2} is lower than the indicated power P_{Ind} in relation to mechanical losses and the power needed for driving appended auxiliary components.

$$P_M = \frac{n_M \cdot z}{30 \cdot \tau} V_s \cdot p_{sr,e} = P_{Ind} \frac{p_{sr,e}}{p_{sr,in}}, \quad (40)$$

$$p_{sr,e} = p_{sr,Ind} - p_{sr,tr}. \quad (41)$$

According to Kochanowsky and Thiele [11] the mean pressure of friction losses $p_{sr,tr}$ includes the effect of friction in the mechanism, effect of driving fuel injection pump and valves, effect of engine load, effect of turbocharging pressure, and effect of cooling water and oil temperature when these values deviate from the nominal ones.

2.11. System of speed regulation

The type of governor applied in this paper is basically an incremental PID speed governor with two stages of freedom of setting the parameters. The output signal of the chosen governor performance is formed following the equation (42).

$$U(s) = K_R [bX_R(s) - Y(s)] + \frac{K_R}{T_I s} [X_R(s) - Y(s)] + \frac{K_R T_D s^2}{1 + \frac{T_D}{v} s} [cX_R(s) - y(s)]. \quad (42)$$

A first order filter for reducing measuring noise has been fitted in the model for revolution speed governor of the propulsion diesel engine. The reduction of effects of impulse interference is obtained by fitting a device for limiting the rate of signal in feedback loop. The method of conditional integration is used for preventing the effect of the integrator windup. In addition, the governor features elements for limiting the movement of the fuel rack φ_g , depending on the speed n_m and scavenge air pressure p_z .

2.12. Fuel pump

The engine considered in this paper is provided with a reciprocating high-pressure pump with a spirally designed rim of the plunger. In order to enhance the combustion process and adjust it to differing fuel quality, a *VIT* system has been fitted which allows changing of the injection timing [12]. The amount of fuel injected into the cylinder depends on the position of the fuel rack and the revolution speed of the engine. For the purposes of this paper, the above mentioned features have been acquired through the digitisation of diagrams provided by the manufacturer and examination at the testbed.

3. The computer-aided simulation model

The MATLAB 7.0.4. – SIMULINK computer application has been used for designing the computer-aided simulation model in this paper. The computer-aided simulation model has been designed on the basis of a mathematical zero-dimensional model. The model is described using a system of non-linear differential equations supplemented by empirical and correlative equations describing the system components and boundary conditions. Using the computer-aided simulation model, the crank angle and real time have been defined with the help of the simulation time, so that all calculated condition variations can be observed through the crank angle and time. Figure 1 presents the block scheme of the designed model for a marine propulsion system. The model consists of eight basic elements that are mutually correlated forming a coherent whole. The basic elements are: *governor and fuel pump, engine cylinders, exhaust receiver, scavenging and charging receiver, turbine, compressor, turbocharger dynamics, and engine mechanism dynamics*. The model enables simulation of operation of ship propulsion systems with a two-stroke slow-speed engine and a fixed blade propeller. It is easy to harmonise the model with various propulsion system designs. Simulation of the model using a computer operating at 1,7 GHz allows the user to obtain simulation time almost equal to real time, on condition that it takes calculation steps starting with 1° of the crankshaft angle, uses the Euler integration method, and that certain number of working parameters have been stored beforehand.

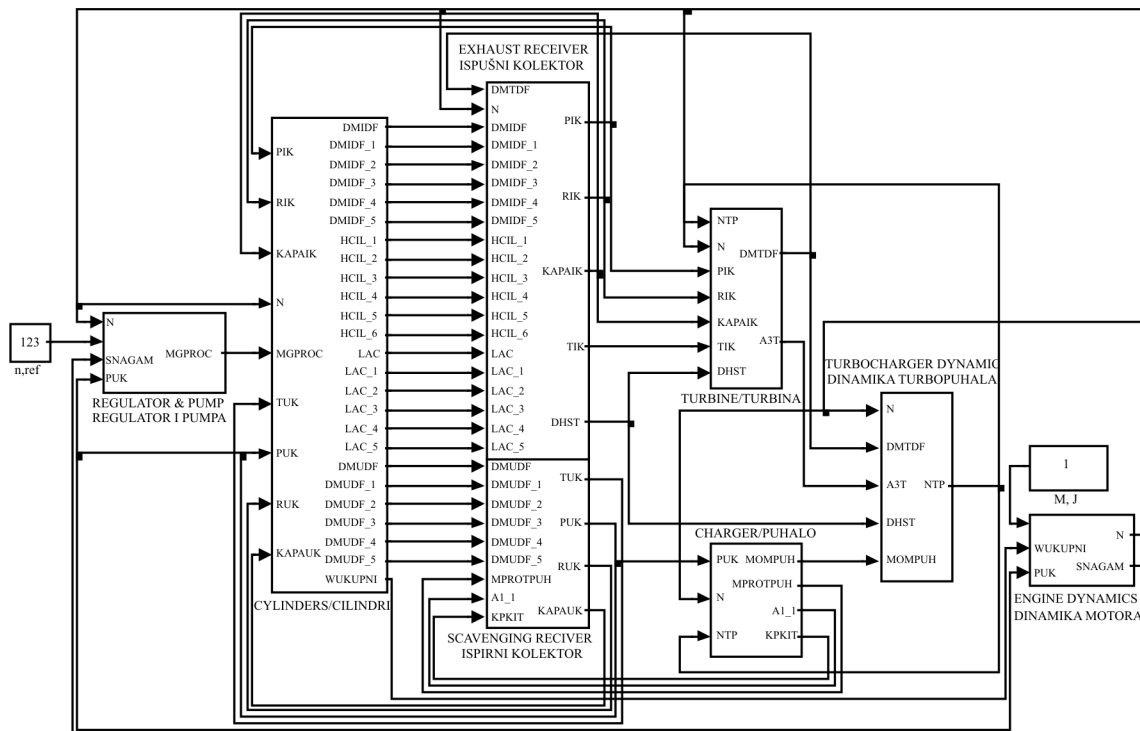


Figure 1. Block scheme of the model for marine propulsion system in the Matlab-Simulink computer program
Slika 1. Blok-shema modela brodskog propulzijskog sustava u Matlab-Simulink računalnoj aplikaciji

For the purposes of a detailed research, in defining the time of the transient processes or the very stages of the cycle within the engine, a smaller calculation step is chosen, e.g. 0.1° , 0.01° etc., as well as a more accurate integration method, e.g. Runge-Kutta method. For starting the simulation the user can choose any operating point after obtaining its starting values by iterative methods.

3.1. Application of the simulation model

The simulation model has been applied on the propulsion system of a chemical tanker, having the following features:

- over-all length 82,90 m,
- breadth 32,20 m,
- draught (design waterline) 12,00 m,
- deadweight 46000 dwt (metric tons).

Basic technical characteristics of the propulsion engine MAN B&W 6S50MC:

- process 2-stroke, direct injection,
- number of cylinders 6 in line,
- cylinder bore 500 mm,
- stroke 1910 mm,

- maximum continuous power 8580 kW,
- maximum continuous speed 127 min^{-1} ,
- maximum mean effective pressure 18 bar,
- maximum combustion pressure 143 bar,
- specific fuel consumption $171 \text{ g/(kW}\cdot\text{h)}$, 100 % load, (with high-efficient turbocharger)
- compression ratio (obtained by calculation) 17,2,
- ratio of the cranking linkage r/l 0,436,
- volume of the exhaust receiver $6,13 \text{ m}^3$,
- volume of the scavenging air receiver $7,179 \text{ m}^3$,
- opening angle of the scavenge channels 40° before BDC,
- closing angle of the scavenge channels 40° after BDC,
- opening angle of the exhaust valve 61° before BDC,
- closing angle of the exhaust valve 80° after BDC,
- mean value of the moment of inertia $28467 \text{ kg}\cdot\text{m}^2$.

Technical features of the turbocharger manufactured by ABB, type *TPL77-B11* are:

- diameter of the compressor rotor 0,699 m,
- external diameter of the turbine rotor 0,4889 m,
- reference flow area of the turbine $0,036263 \text{ m}^2$,
- maximum revolution speed 304 s^{-1} ,
- polar moment of inertia of the rotor $3 \text{ kg}\cdot\text{m}^2$.

Technical features of the ship's propeller:

- number of propeller blades 4
- diameter of the propeller 5,550 mm,
- pitch 7,870 mm,
- overall moment of inertia 27250 kg·m².

The model's validity has been examined for stationary operating points at: 25 %, 50 %, 75 %, 93,5 %, 100 % and 110 % of the load. The data have been obtained by starting the simulation model under a 100 % load. After that, the operating parameters for other observed loads were obtained through the change of the set revolution speed, i.e. the amount of fuel. Looking at Figure 2, we can notice that the deviations between the measured values and the ones obtained by the simulation are minimal.

The temperature of air at the compressor suction is practically within the interval range (5,45) °C. Figure 3 presents specific fuel consumption, temperature and pressure in the exhaust gas and scavenge air receivers, for various air temperatures at the compressor suction. The diagram has been obtained on the simulation model under maximum continuous rating (MCR). The results of the simulation refer to the reference temperature at the compressor inlet, as well as to temperatures increased and reduced by 5 and 20 °C, which would correspond to extreme conditions. In the event of lower temperature at the compressor suction, the air mass flow through the compressor is greater, so that the mass in the scavenge air receiver is greater as well. The temperature after the

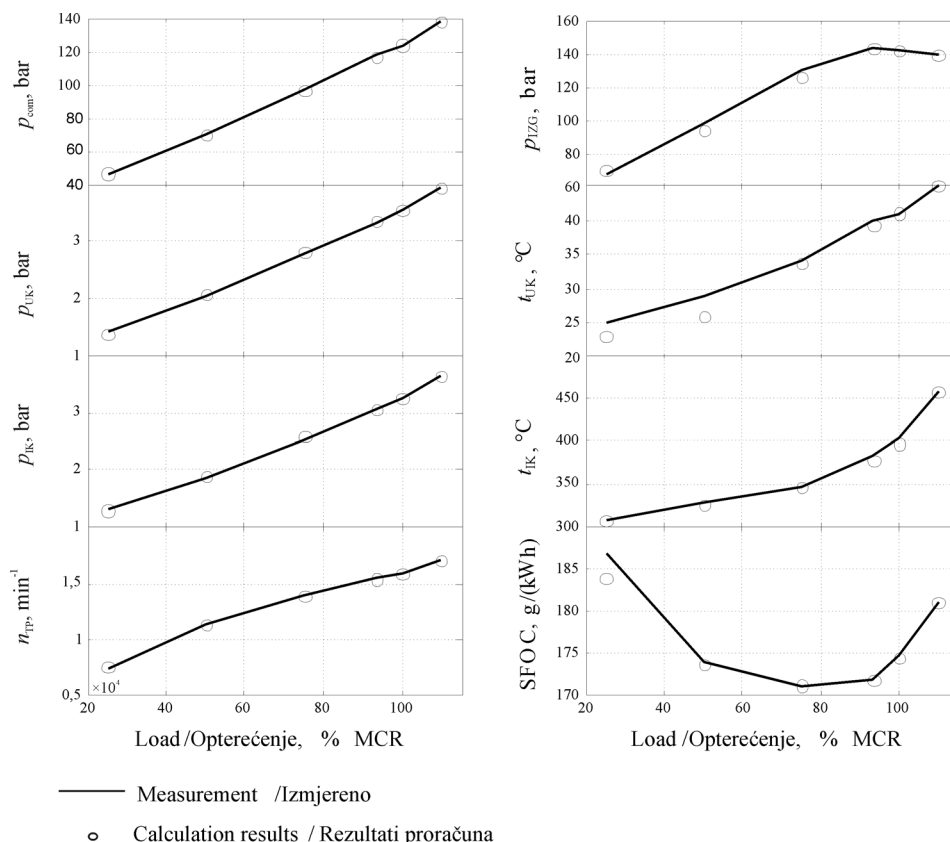


Figure 2. Comparison of the measured values and the results of the simulation at stationary points at: 25 %, 50 %, 75 %, 93,5 %, 100 % and 110 % of the engine load

Slika 2. Usporedba izmjerenih vrijednosti i rezultata simulacije u stacionarnim točkama, pri: 25 %, 50 %, 75 %, 93,5 %, 100 % i 110 % opterećenja motora

3.2. Analysis of engine and turbocharger performance under aggravated conditions on the simulation model

This paper analyses the performance of the engine and turbocharger at various air temperatures at the compressor suction, with dirty turbine blades, under varying external loads due to heavy sailing conditions in rough seas.

cooler is increased. According to Figure 3, in the event of the compressor suction temperature reduced by 20 °C, the scavenge air pressure is increased by 0,265 bar. The temperature of the cylinder is also increased by 4,81 °C. The compression pressure is increased due to a higher pressure of the air for scavenging the cylinders.

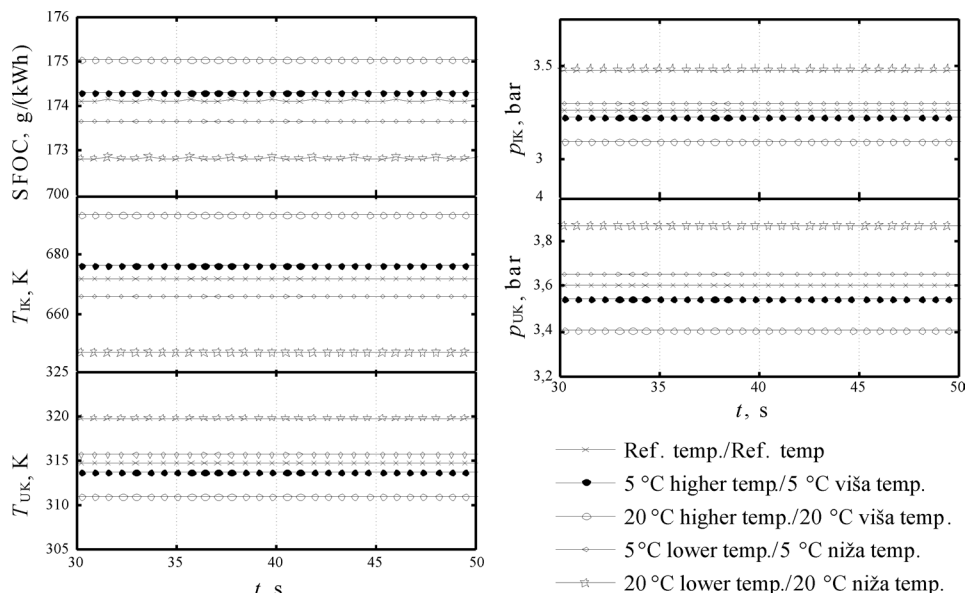


Figure 3. Specific consumption of fuel, temperature and pressure in the exhaust and scavenge air receivers for various air temperatures at the compressor suction

Slika 3. Specifična potrošnja goriva, temperature i tlak u kolektoru ispušnih plinova i ispirog zraka, za različite temperature zraka na usisu turbopuhala

Figure 4 shows the same example, featuring the compression pressure increased by 11,3 bar. The increased compression pressure results in higher positive work per cycle, so that the fuel consumption is lower by 0,79 % under the same engine load. The temperature of cylinder gases is decreased by 63 °C with regard to the referential one, due to combustion of the lower amount

of fuel. The lower temperature of the cylinder process results in exhaust gas temperature reduced by 24 °C. The pressure in the exhaust receiver is higher because of an increased amount of exhaust gases, which is the result of a higher pressure during the process of scavenging the engine cylinders.

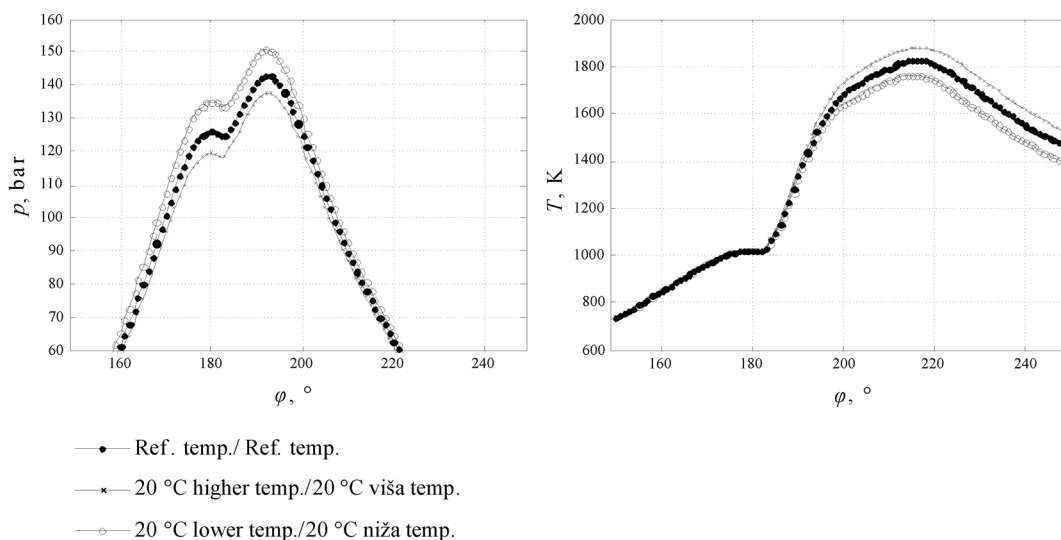


Figure 4. Pressure and gas temperature in the engine cylinder during upper part of the cycle, at various air temperatures at the compressor suction

Slika 4. Tlak i temperature plinova u cilindru motora, za vrijeme gornjeg dijela ciklusa, za različite temperature zraka na usisu turbopuhala

Figure 5 presents cylinder gas pressure rates during scavenging at various air temperatures at the compressor suction. If the air temperature at the compressor inlet is higher than the referential one, Figures 3-5 show changes similar to the described example with reduced temperature, but the sign is reversed.

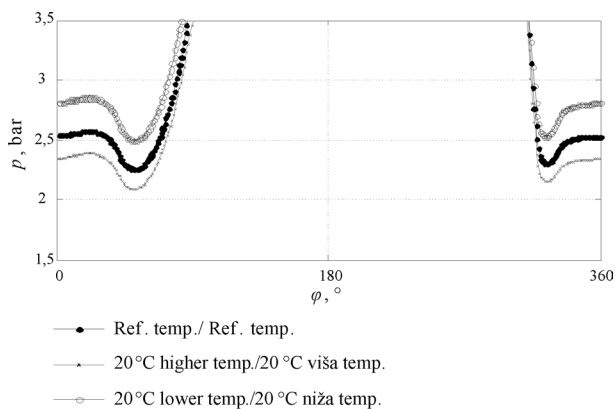


Figure 5. Gas pressures in the engine cylinder during scavenging, at various air temperatures at the compressor suction

Slika 5. Tlakovi plinova u cilindru motora tijekom faze ispiranja, za različite temperature zraka na usisu puhala

Figure 6 shows the change of the compressor’s operating point when simulating engine load change in heavy seas and at various air temperatures at the compressor suction. The figure presents the results of the simulation for referential conditions. If the air temperature at the compressor suction is increased by 20 °C, it is noticed that the compressor’s operating points are placed lower than in the reference example. Due to the reduction of the pressure ratio before and after the compressor, and because of the lower revolution speed, the volume of air flow decreases. If the air temperature at the compressor suction is decreased by 20 °C, it is noticed that under the same load changes, the compressor supplies a greater amount of air and it operates more efficiently, but the operating range approaches the surging limit.

Turbines in marine engines using heavy fuel oil are exposed to sediment formation. This reduces the flow area of the nozzle ring, as well as the efficiency, which affects the engine and turbocharger performance. The measurement results, obtained from the manufacturer of the turbocharger considered in this paper, show the connection between the reduction of the nozzle ring flow area and the increase of losses that reduce turbine efficiency. The function obtained by measurement is not linear. Figures 7, 8 and 9 present the results of the

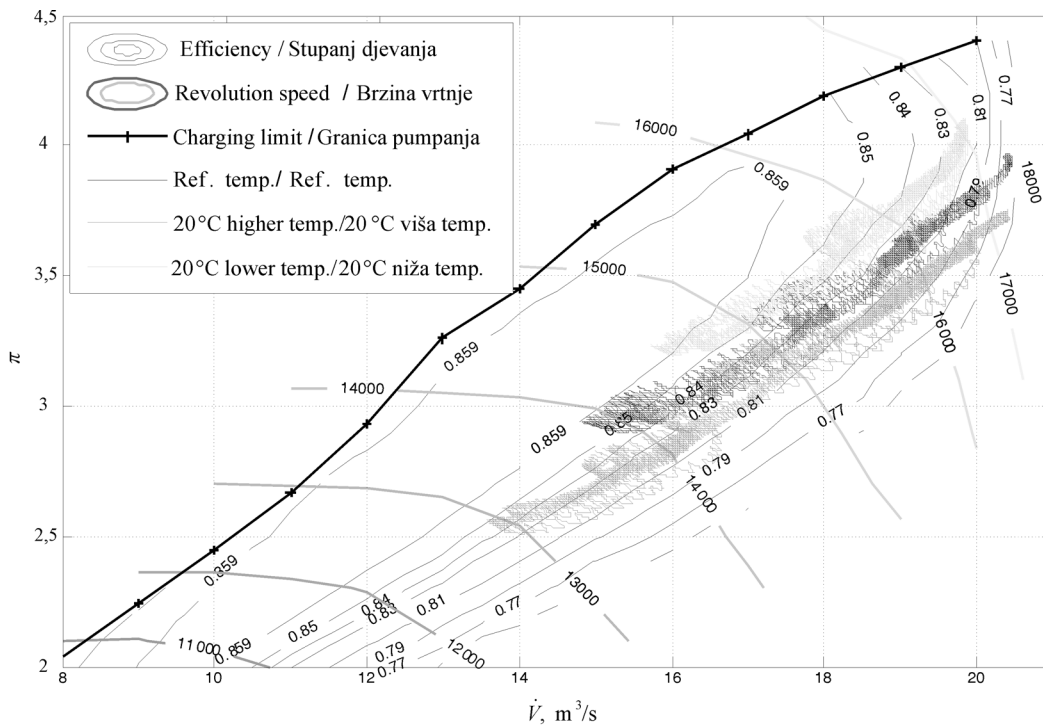


Figure 6. Change of compressor operating point when simulating engine load in heavy seas, at various air temperatures at the compressor suction

Slika 6. Promjena radne točke puhala za vrijeme simulacije opterećenja motora na veoma valovitom moru, za različite temperature zraka na usisu turbopuhala

simulation of the turbocharged engine operation with a turbocharger whose nozzle ring flow area has been reduced by 15 % with regard to the referential one, and with turbine efficiency additionally reduced by 10 % with regard to the referential one.

so that the entire process occurs at a somewhat higher temperature. In addition, the specific fuel consumption is increased and a higher amount of heat energy is released in the engine cylinder, which increases the temperature of gases in the engine cylinder. According to Figure 8, an

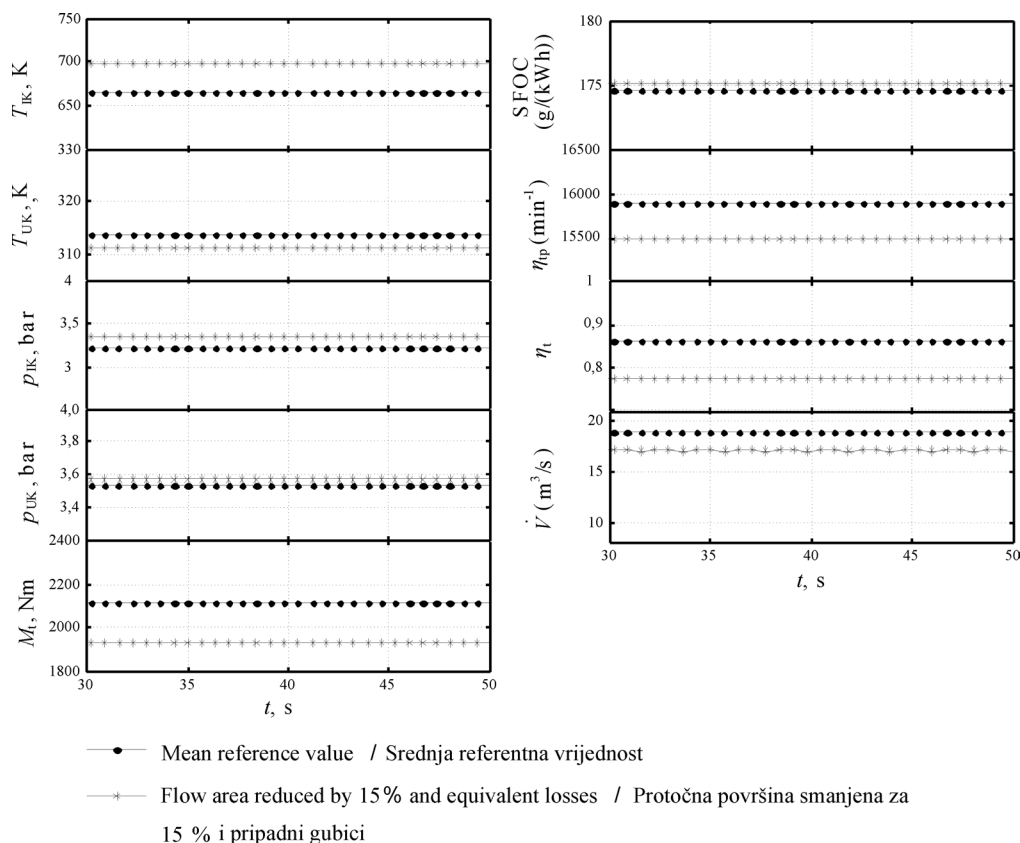


Figure 7. Engine performances under 100 % load, for referential parameters and for a contaminated turbine with a flow area reduced by 15 % and equivalent losses

Slika 7. Značajke motora pri 100 % opterećenju, za referentne značajke i za onečišćenu turbinu sa smanjenom protočnom površinom za 15 % i ekvivalentnim gubitcima

The pressure rise in the exhaust receiver, caused by smaller flow area, has been reduced due to the effect of decreased efficiency. Increased losses cause the reduction of torque on the turbocharger shaft, which leads to a decreased revolution speed, so that the volume air flow is lower than the referential one by 11 %. Because of a lesser air flow through the cooler, the air temperature in the scavenge receiver is lower. Hence the air mass is increased, which results in almost unchanged pressure in the scavenge air receiver. Due to the increased pressure and temperature in the exhaust gas receiver, temperature rises during the scavenging process of working fluid,

analysis of the pressure diagram in the cylinder shows a slight compression pressure rise, due to a slight pressure rise during the scavenging stage. Contamination of the turbocharger adversely affects the engine's performance. The specific fuel consumption is higher and the engine is more exposed to overheating. It operates with a lower air excess ratio in the cylinders, which increases the possibility of incomplete combustion and accelerates the process of further contamination of the turbine with soot. The contamination of the turbine significantly affects the compressor's operation.

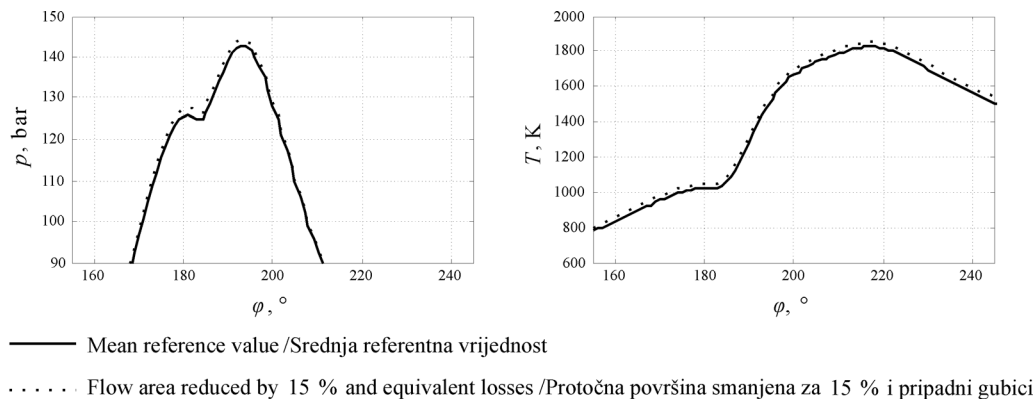


Figure 8. Pressure and temperature in the engine cylinder, under 100 % load, for referential parameters, and for a contaminated turbine with a flow area reduced by 15 % and with equivalent losses

Slika 8. Tlak i temperatura u cilindru motora, pri 100 % opterećenju, za referentne značajke i za onečišćenu turbinu sa smanjenom protočnom površinom za 15 % i ekvivalentnim gubitcima

Figure 9 shows the variation of the compressor’s operating point during simulation of the engine load change in heavy seas, for both clean and contaminated turbine. The analysis of the results has ascertained that the compressor’s operating point in the event of contamination of the turbine, which is shown in grey colour, has almost reached the surging limit of the compressor. When the turbine is contaminated, the torque and revolution speed

of the turbocharger shaft is reduced, which results in a decrease of the air volume flow. Meanwhile, pressure ratio before and after the compressor remains almost steady, so that, within the area of the compressor features, operating points are shifted towards the left, with regard to the results of the simulation on a clean turbine, shown in black colour on Figure 9.

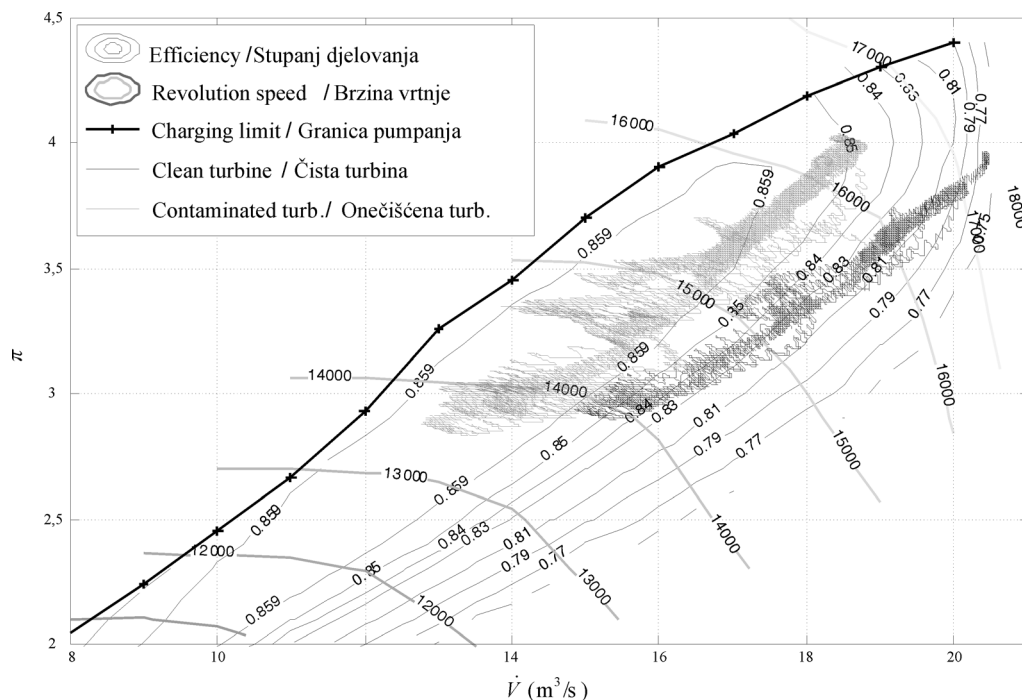


Figure 9. Variation of the compressor’s operating points during the simulation of the engine load in heavy seas, for clean and dirty turbines

Slika 9. Promjena radne točke puhalo za vrijeme simulacije opterećenja motora na veoma uzburkanom moru za slučaj čiste i onečišćene turbine

4. Conclusion

In this paper a zero-dimensional model has been designed for assessing the quality and reliability of the diesel engine propulsion system under aggravated conditions. The model consists of components whose mathematical descriptions have been derived from basic laws of mechanics, thermodynamics, heat transfer and fluid dynamics, mutually correlated by flows for the transfer of mass and energy. The numerical model has been implemented on the computer using the application MATLAB 7.0.4. – SIMULINK. By applying some modifications and entering appropriate parameters, the proposed simulation model can be applied to any propulsion system with a two-stroke diesel engine with turbocharging and uniflow scavenging of the cylinders. In this paper the simulation model has been applied for analysing a diesel engine propulsion system consisting of a two-stroke slow-speed turbocharged diesel engine and a fixed blade propeller. The model's examination revealed a close correspondence between the designed and the measured engine's performance at the testbed, for stationary operating points in a wide load range from 25 % to 110 %. In addition to referential environment conditions, an analysis of the engine and turbocharger performance at various air temperatures at the compressor suction and under maximum continuous rating has been made. If the temperature at the compressor suction drops by 20 °C, the scavenge air pressure increases by 0,265 bar, and its temperature by 4,81 °C. Compression pressure rises by 11,3 bar, resulting in a better positive work of the cycle, with fuel consumption reduced by 0,79 %. Maximum temperature during the process is decreased by 63 °C with regard to the referential one, so that the exhaust gas temperature is lower as well by 24 °C. In the event of the air temperature at the compressor suction reduced by 20 °C, air supply rises significantly and the compressor operates more efficiently, but the operating point approaches the surging limit. If the air temperature at the compressor inlet is higher than the referential one, similar changes occur, but the sign is reversed.

Applying the model presented in this paper the impact of contamination of the turbine on the engine and turbocharger performance has been also investigated. At the flow area reduced by 15 %, with efficiency reduced by 10 %, the compressor's operating point approaches the surging limit. At the same time the backup air supply to the engine is reduced by half, with regard to the referential conditions when using a clean turbine. When analysing the results of the simulation of the engine performance in heavy seas, and in the event of contamination, the compressor's operating point reaches the surging limit.

REFERENCES

- [1] HEIM, K.: *Existing and Future Demands on the Turbocharging of Modern Large Two-stroke Diesel Engines*, The 8th Supercharging Conference 1-2 October 2002, Dresden.
- [2] RAČIĆ, N.: *Simulacija rada brodskog propulzijskog sustava sa sporohodnim dizelskim motorom u otežanim uvjetima*, disertacija (engl.: Simulation of performance of the marine slow-speed diesel propulsion engine under aggravated conditions, Ph. D. Thesis), Tehnički fakultet Rijeka, University of Rijeka, 2008.
- [3] MEDICA, V.: *Simulacija dinamičkih uvjeta rada dizelmotora s prednabijanjem kod pogona električnog generatora* (engl.: Simulation of Turbocharged Diesel Engine Driving Electrical Generator under Dynamic Working Conditions, Ph. D. Thesis), Tehnički fakultet Rijeka, University of Rijeka, 1988.
- [4] RADICA, G.: *Ekspertni sustav za dijagnostiku stanja i optimiranje rada brodskog diesellovog motora* (engl.: Expert System for Diagnosis and Optimisation of Marine Diesel Engine, Ph. D. Thesis), Sveučilište u Zagrebu, University of Zagreb, 2004.
- [5] HOHENBERG, G.: *Advanced approaches for Heat Transfer Calculation*, SAE Paper 790825, 1979.
- [6] WOSCHNI, G.; ANISITS, F.: *Eine Methode zur Vorausberechnung der Änderung des Brennverlaufes mittelschnellaufender Dieselmotoren bei geänderten Betriebsbedingungen*, MTZ 34 (1974) 4, 106-115.
- [7] SITKEI, G.: *Kraftstoffaufbereitung und Verbrennung bei Dieselmotoren*, Springer Verlag, Berlin, 1964.
- [8] BENSON, R.S.; BRANDHAM, P.J.: *A method for obtaining a quantitative assessment of the influence of charge efficiency on two-stroke engine performance*, Int. J. Mech. Sci. 11, (1969), 303.
- [9] BOY, P.: *Beitrag zur Berechnung des instationären Betriebsverhaltens von mittelschnellaufenden Schiffsdieselmotoren*, Dissertation, Hannover: TH, 1980.
- [10] PFLAUM, W.; MOLLENHAUER, K.: *Wärmeübergang in der Verbrennungs-kraftmaschine*, Springer Verlag, Wien, 1977.
- [11] KOCHANOWSKI, H. A.; Thiele, E.: *Motorreibung - Ermittlung und Erfassung der mechanischen Verluste in Verbrennungsmotoren*, Vorhaben Nr. 133 und 176 FVV 1. Teilabschlussbericht 1977.
- [12] ...: *MAN Diesel A/S: The MAN B&W Engine VIT Fuel Pump*, Technical Papers, Copenhagen, Denmark, 2004.